

Highly sensitive spectroscopic detection of heme-protein submonolayer films by channel integrated optical waveguide

Ismail Emre Araci¹, Sergio B. Mendes^{1,2}, Nasuhi Yurt¹, Seppo Honkanen^{1,3},
and N. Peyghambarian¹

¹College of Optical Sciences, The University of Arizona, 1630 E. University Blvd., Tucson, AZ, U.S.A. 85721

²Department of Physics and Astronomy, University of Louisville, Louisville, KY, U.S.A. 40292

³Micro and Nanosciences Laboratory, Helsinki University of Technology, Finland, 02015 TKK

Abstract: A highly sensitive technique based on optical absorption using a single-mode, channel integrated optical waveguide is described for broad spectral band detection and analysis of heme-containing protein films at a glass/water interface. Fabrication steps and device characteristics of optical waveguides suitable for operation in the wavelength range of 400 - 650 nm are described. Experimental results reported here show a limit of detection smaller than 100 pg/cm² for a submonolayer of ferricytochrome *c* by probing the Soret transition band with a 406-nm semiconductor diode laser propagating in a single-mode, ion-exchanged channel waveguide. By taking advantage of the exceptionally low limit of detection, we examined the adsorption isotherm of cytochrome *c* on a glass surface with unprecedented detail. Unlike other surface-specific techniques (e.g. SPR, integrated optic Mach-Zehnder interferometer) that probe local refractive-index changes and therefore are very susceptible to temperature fluctuations, the integrated optical waveguide absorption technique probes molecular-specific transition bands and is expected to be less vulnerable to environmental perturbations.

©2007 Optical Society of America

OCIS codes: (130.6010) Sensors; (230.7380) Waveguides, channeled; (130.2790) Guided waves.

References and links

1. J. D. Swalen, D. L. Allara, J. D. Andrade, E. A. Chandross, S. Garoff, J. Israelachvili, T. J. McCarthy, R. Murray, R. F. Pease, J. F. Rabolt, K. J. Wynne, and H. Yu, "Molecular Monolayers and Films," *Langmuir* **3**, 932-950 (1987).
2. J. Homola, S. S. Yee, and G. Gauglitz, "Surface plasmon resonance sensors: review," *Sens. Actuators B* **54**, 3-15, (1999).
3. W. D. Wilson, "Analyzing biomolecular interactions," *Science* **295**, 2103-2105, (2002).
4. Biocore Product Brochure, "Biacore 3000," (2007).
http://www.biocore.com/lifesciences/products/systems_overview/3000/system_information/index.html
5. A. F. Runge, N. C. Rasmussen, S. S. Saavedra, and S. B. Mendes, "Determination of anisotropic optical constants and surface coverage of molecular films using polarized visible ATR spectroscopy. Application to adsorbed cytochrome *c* films," *J. Phys. Chem. B* **109**, 424-431 (2005).
6. S. B. Mendes, L. F. Li, J. J. Burke, J. E. Lee, D. R. Dunphy, S. S. Saavedra, "Broad-band attenuated total reflection spectroscopy of a hydrated protein film on a single mode planar waveguide," *Langmuir* **12**, 3374-3376 (1996).
7. J. T. Bradshaw, S. B. Mendes, and S. S. Saavedra, "A Simplified Broadband Coupling Approach Applied to Chemically Robust Sol-Gel, Planar Integrated Optical Waveguides," *Anal. Chem.* **74**, 1751 - 1759 (2002).
8. I. H. A. Badr and M. E. Meyerhoff, "Fluoride-selective optical sensor based on Aluminum (III)-octaethylporphyrin in thin polymeric film: further characterization & practical application," *Anal. Chem.* **77**, 6719-6728 (2005).
9. T. Umemura, H. Hotta, T. Abe, Y. Takahashi, H. Takiguchi, M. Uehara, T. Odake, K. Tsunoda, "Slab optical waveguide high-acidity sensor based on an absorbance change of protoporphyrin IX," *Anal. Chem.* **78**, 7511-7516 (2006).

10. Y. Itagaki, K. Deki, S. I. Nakashima, Y. Sadaoka, "Development of porphyrin dispersed sol-gel films as HCl sensitive optochemical gas sensor," *Sens. Actuators B* **117**, 302-307 (2006).
11. Y. Y. Cheng, S. H. Lin, H. C. Chang, M. C. Su, "Probing adsorption, orientation and conformational changes of cytochrome c on fused silica surfaces with the Soret band," *J. Phys. Chem. A* **107**, 10687-10694 (2003)
12. S. B. Mendes and S. S. Saavedra, "Comparative Analysis of Absorbance Calculations for Integrated Optical Waveguide Configurations by use of the Ray Optics Model and the Electromagnetic Wave Theory," *Appl. Opt.* **39**, 612-621 (2000).
13. A. Tervonen, P. Poyhonen, S. Honkanen, M. Tahkokorpi, S. Tammela, "Examination Of 2-Step Fabrication Methods For Single-Mode Fiber Compatible Ion-Exchanged Glass Wave-Guides," *Appl. Opt.* **30**, 338-343 (1991).
14. W. Lukosz, "Integrated Optical Chemical and Direct Biochemical Sensors," *Sens. Actuators B* **29**, 37-50 (1995).
15. S. Honkanen, "Silver-Film Ion-Exchange Technique," in *Introduction to Glass Integrated Optics*, S. I. Najafi, ed., (Artech House, Boston-London, 1992).
16. R. W. Chuang and C. C. Lee, "Low-loss deep glass waveguides produced with dry silver electromigration process," *J. Lightwave Technol.* **20**, 1590-1597 (2002).
17. R. A. Scott and A. G. Mauk, in *Cytochrome c: A Multidisciplinary Approach*, (University Science Books, Sausalito, CA, 1996).
18. E. Margoliash and N. Frohwirt, "Spectrum of Horse-Heart cytochrome c," *Biochem. J.* **71**, 570-572 (1959).
19. P. Poyhonen, S. Honkanen, A. Tervonen, M. Tahkokorpi, and J. Albert, "Planar 1/8 Splitter in Glass by Photoresist Masked Silver Film Ion-Exchange," *Elect. Lett.* **27**, 1319-1320 (1991).
20. J. Viljanen and M. Leppihalme, "Analysis of Loss in Ion-Exchanged Glass Waveguides," *Proc. European Conf. Integrated Optics*, (Institution of Electrical Engineers, London, 1981), pp.18-21.
21. S. Honkanen and A. Tervonen, "Experimental-analysis Of Ag⁺-Na⁺ Exchange in Glass with Ag Film Ion Sources for Planar Optical Wave-Guide Fabrication," *J. Appl. Physics* **63**, 634-639 (1988).
22. M. Leone, A. Cupane, V. Militello, and L. Cordone, "Thermal broadening of the Soret band in heme complexes and in heme proteins: role of the iron dynamics," *Eur. Biophys. J.* **23**, 349-352 (1994).
23. A. F. Runge and S. S. Saavedra, "Comparison of microcontact-printed and solution-adsorbed cytochrome c films on indium tin oxide electrodes," *Langmuir* **19**, 9418-9424 (2003).

1. Introduction

Binding characteristics of proteins at various interfaces are critical for a wide range of biotechnological fields and play a key role in the development/screening of novel pharmaceutical drugs [1]. Over the past decade, highly sensitive optical techniques for investigating biological films has been widely used for real-time monitoring of molecular interactions at bio-interfaces; most prevalent among these techniques has been surface plasmon resonance (SPR) [2-4]. In the SPR technique, molecular adsorption at the probing interface creates a local change in the refractive index inside the evanescent-field region of the plasmon mode that translates into a shift of the resonant angle. An angular shift of approximately 1×10^{-4} of a degree corresponds typically to the adsorption of a protein film of approximately 100 pg/cm^2 [3, 4]. Besides the high angular resolution needed by the SPR technique, an exceptional temperature/mechanical control is also required to prevent refractive-index perturbations from the bulk phase into the surface plasmon mode.

Transduction in protein films by broadband or multi-wavelength optical absorption using planar integrated optical waveguides can potentially simplify analyte detection and identification, due to its spectral specificity and robustness against environmental changes. A chromophore located within the evanescent region interacts with the guided electromagnetic radiation and thus attenuates its optical intensity; such an approach using planar slab single-mode waveguides have been used for investigations of physical/chemical properties of surface-adsorbed proteins in the middle of the visible spectral region [5, 6]. However, to take full advantage of the higher extinction coefficient at the Soret band in heme-proteins and reach a limit of detection (LOD) at least comparable or superior to SPR, single-mode channel waveguides operating in the 400-nm range with low loss are needed. In that perspective, a slab waveguide spectrometer that transmitted light down to 400 nm was demonstrated previously [7]. However, light intensity in the 400-nm region was only marginal, and thus stray light and low signal-to-noise ratio (SNR) were crucial factors that hampered the limit of detection in that work. In addition, there has been great interest in using the Soret transition

band as a sensing probe for both protein and chemical measurements as described in many works such as polymer-film based fluoride sensor [8], glass-slide optical waveguide acidity sensor [9], gas phase HCl sensor based on sol-gel film [10], and detection of protein adsorption by attenuated total reflection [11].

By using a silver-film ion-exchange process, we developed here highly confined, single-mode, integrated optical waveguides that exhibit sufficiently low propagation loss in the short wavelength range and provide high detection sensitivity; in addition this work employs channel waveguides which is a superior configuration to interface the probing device with fiber coupled sources and detectors when compared to slab waveguides. These glass waveguides, which provide low optical losses and are fairly inexpensive, can potentially enable the fabrication of miniature disposable integrated optical biosensors. To demonstrate the strong optical response and much improved LOD in our waveguides, a submonolayer film of the protein ferricytochrome c (cyt c) was utilized. Due to the superior SNR in our setup, the adsorption isotherm of cyt-c molecules on a glass/aqueous interface was examined with unprecedented detail, and LOD results were determined from the measured SNR and absorbance values.

2. Preliminary considerations

It is well known that attenuation of guided modes due to the presence of chromophores in the evanescent region strongly depends on the waveguide geometry and that a single-mode configuration provides the maximum sensitivity. The evanescent field absorption in optical waveguides follows a pseudo Lambert-Beer relationship and, for chromophores bound to the waveguide surface, the absorbance A is given by [12]:

$$A = (\varepsilon \Gamma l) \times \kappa / h \quad (1)$$

where ε is the molecular extinction coefficient, Γ is the molecular surface density (surface coverage), l is the optical interaction length, κ is the fraction of the normalized waveguide mode profile occupied by the adsorbed molecular film, and h is the thickness of the adsorbed film. Fig. 1(a) shows the schematic of the absorption-based sensing with a single-mode planar optical waveguide.

Glass integrated optic represents a viable approach for the development of inexpensive and robust passive biosensor devices. Binary ion-exchange, in turn, is one of the most widespread technologies for the fabrication of optical waveguides in glass substrates. Ag^+ - Na^+ ion-exchange glass waveguides have been used for fabrication of passive optical devices for telecommunication applications in the 1.3-1.5 μm region exhibiting low propagation loss and fiber-to-waveguide coupling loss [13]. However, low-cost fabrication of single-mode waveguides at wavelengths lower than 450 nm has been a challenge due to increased waveguide losses and smaller dimensions required at lower wavelengths. Another challenge to efficiently take advantage of ion-exchange waveguides for optical sensing has been the need of a high contrast refractive-index profile for increased mode confinement and thus higher sensitivity [14]. Based on these considerations, we have chosen a silver film technique for fabrication of the ion-exchanged waveguides [15, 16].

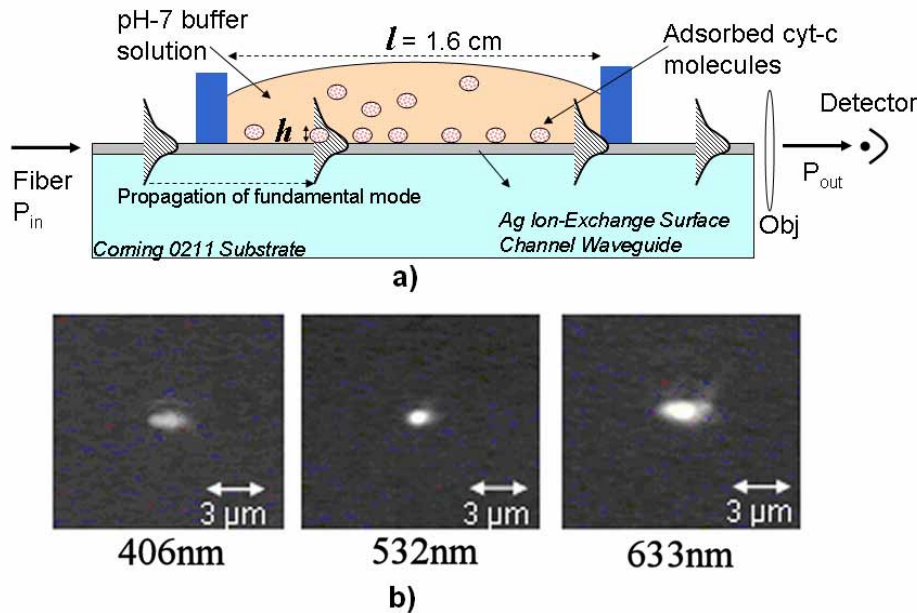


Fig. 1. (a). The schematic of the waveguide sensing platform. The fundamental mode of Ag ion exchange waveguide interacts with the surface adsorbed cyt c molecules for a pathlength of $l = 1.6$ cm. Interaction strength, κ , is determined by h and evanescent tail of the mode as shown. (b) Near field images of the waveguide output. Only the fundamental mode was excited at 532 nm. Superposition of two lateral modes can be seen for 406 nm.

The cyt c protein was used as a biomolecular film in our model tests [5, 6, 11, 17, 18]. Cyt c is a small stable protein that can reversibly withstand rather extreme conditions and has been used in several studies of protein mechanisms [17]. The prosthetic heme group in cyt c is a useful spectroscopic probe as it strongly absorbs in the UV and visible regions. As previously reported [18], oxidized cyt c has a strong optical absorption at the Soret band centered at 410 nm, and a weaker and broader absorption band located at 528 nm. The detection enhancements that were made possible by improvements on the fabricated waveguides were demonstrated by utilizing two different wavelengths (406 nm and 532 nm) to probe the binding of cyt c molecules to the glass waveguide surface, while a 633-nm wavelength which is outside the protein transition bands was used to monitor device stability. Waveguide sensitivity is strongly dependent on polarization when the film thicknesses are close to the waveguide cutoff range [14]. However, we operated significantly away from cut-off conditions for both polarizations and modeling results indicated that the effects of polarization were not significant in our case.

3. Waveguide fabrication and characterization

The waveguide fabrication was done on 0.5-mm-thick Corning 0211 glass substrates, which is known to be optically transparent above 320 nm and has a refractive index of $n_{subs} = 1.52$. A photoresist film with 3 μm openings was used for masking during the ion exchange process to form channel waveguides [19]. Ag film with 100-nm thickness was deposited on the patterned samples. For the silver film technique, previous works have reported extremely high propagation losses around 450 nm due to the formation of small Ag particles just beneath the glass surface [15]. The reported loss value even for a highly multimode (depth: 20 μm , width: 40 μm) ion-exchange waveguide was 6.5 dB/cm at 450 nm [20]. By using a low temperature ion exchange process and by applying a high potential difference, we have minimized the formation of Ag colloidal particles and created waveguides with a step-like index profile. The

ion-exchange process was performed at 105° C for 6.5 hours and during the ion exchange process a potential difference of 980 V was applied between the substrate electrodes to drive Ag^+ ions released from the film into the glass. Next, the substrates were diced into 2.3×2.3 cm² samples and their end facets were polished to increase coupling efficiency. As shown in Fig. 1(a), the optical interaction length was determined by a liquid reservoir that was attached to the waveguide surface with a UV-curable epoxy. The refractive index of the epoxy, n_{epoxy} , was chosen to be smaller than n_{subs} to preserve the waveguiding condition. The fabricated waveguides were characterized at several wavelengths. A laser diode with current and temperature controllers, a diode-pumped solid state frequency-doubled laser, and a He-Ne laser were used as light sources at 406, 532, and 633 nm, respectively. A microscope objective at the end of the waveguide was used to image waveguide output to a detector or a camera. At 406, 532, and 633 nm the measured propagation losses were about 8, 3, 2 dB/cm, respectively and the coupling loss was found to be about 8 dB/facet. Figure 1(b) shows the near field images of the waveguide output at different wavelengths. In the direction perpendicular to the sample plane (vertical direction), single-mode operation was clearly observed at all wavelengths. In the lateral direction, depending on the input coupling, a superposition of the first two modes could be excited at 406 nm. Since we have used a single-mode fiber at 406 nm at the input port, the coupling efficiency to the fundamental mode could be made higher compared to the higher-order lateral mode.

4. Surface preparation.

Unless otherwise stated, a pathlength in the waveguide device of $l = 1.6$ cm was used for probing; baseline was acquired when the probing region was covered with an optically transparent 1-mL solution of a 10-mM pH-7 phosphate buffer [see Fig. 1(a)]. Under room temperature, another 1 mL of a cyt c solution in pH-7 phosphate buffer was injected into the sensing region and let adsorb from the bulk aqueous phase onto the waveguide surface; protein binding to the waveguide surface was monitored in real time. The adsorption process is considered to occur mostly because of the electrostatic forces between a negatively charged glass surface and positively charged cyt c molecules [5]. Between each measurement the surface was cleaned with Alconox[®] and distilled water, and dried by blowing air. Previous report by Runge et. al. on cyt c at glass/water interfaces has shown that the protein film saturates on a glass surface at a maximum surface concentration of about $\Gamma = 140$ ng/cm² (molecular weight of cyt c ~13,000), which corresponds to approximately one half of a closely-packed full monolayer [5].

5. Results and discussion

5.1 Simulation results

We have used an in-house software for calculation of mode intensity overlap and waveguide optical response [13]. The simulations were realized for TE polarized light with a cladding index of $n_{\text{clad}} = 1.33$ (for a typical aqueous solution) and the perturbation of the adsorbed film on the mode shape was assumed negligible [12]. For the given fabrication parameters, we have considered $\Delta n_{\text{max}} = n_{\text{subs}} - n_{\text{surface}} = 0.05$ in our modeling [21]. Figure 2 shows the silver ion concentration and the fundamental mode field intensity profile at 406 nm for the fabrication parameters given in waveguide fabrication section.

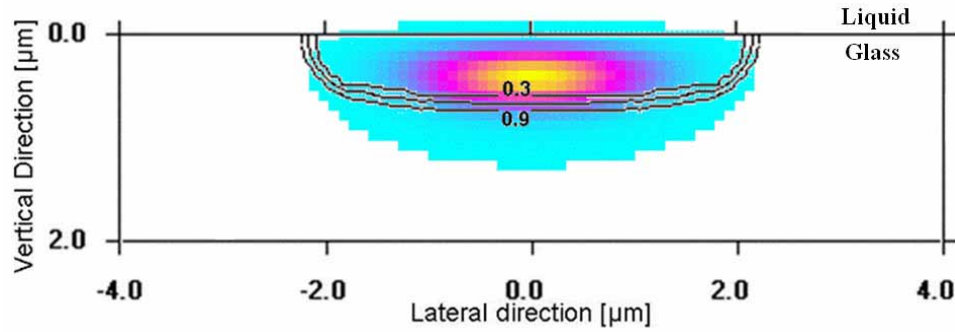


Fig. 2. The silver ion concentration and fundamental mode intensity profile (the solid contour lines are for normalized concentrations of 0.3 0.6 and 0.9 and colors from blue to yellow are for increasing intensity).

At the 532-nm and 633-nm wavelengths, the numerical calculations showed a single-mode operation for both the vertical and lateral confinements, while at 406 nm the structure supports a single-mode structure in the vertical direction and two modes in the lateral direction. In addition, our simulations showed negligible difference in the optical response of different lateral modes at the wavelengths of interest. The step-index profile is clearly seen for ion concentrations shown in Fig. 2 and the effective thickness of the waveguide is less than $1\mu\text{m}$. Intensity profile in Fig. 2 is in visual agreement with experimental data shown in Fig. 1(b). The fraction of the normalized fundamental waveguide mode in the cladding was calculated for 406 nm and found to be 0.63%, and the fraction of this mode overlapping with an adsorbed molecular film of thickness $h = 3\text{ nm}$ (typical size of cyt c), κ was calculated to be 0.032%. This overlap can be directly translated into device response by using the absorbance equation given as Eq. (1). The extinction coefficient of oxidized cyt c is $\epsilon = 95 \times 10^3$ and 11×10^3 $[\text{M} \times \text{cm}]^{-1}$ at 406 and 532 nm, respectively [18]. The resulting absorbance values are $A = 2.25$ and 0.29 at 406 and 532 nm, respectively for an interaction length of $l = 1.6\text{ cm}$ and for a saturated surface concentration of $\Gamma = 140\text{ ng/cm}^2$.

5.2 Experimental results

The adsorption of the molecules was monitored in real-time by continuously detecting the waveguide output intensity. In order to reduce noise in the detected signal, a chopper and a lock-in amplifier were utilized. Figure 3 is the experimental data showing the change in the waveguide output intensity when $10\text{ }\mu\text{M}$ cyt c, which is more than the required concentration to saturate the waveguide surface, was introduced into the sensing area. The absorbance values measured at 406 and 532 nm are 2.1 and 0.25 (in absorbance units) respectively. These values are in good agreement with theoretical calculations given in previous section. Almost an order of magnitude improvement was obtained in the optical response by tuning to the Soret band of cyt c. Although there is negligible optical response at 633 nm for the current analyte, we have used this wavelength to monitor possible effects of mechanical/thermal perturbations due to analyte injection. No change at the 633-nm confirmed the good stability of the experimental setup.

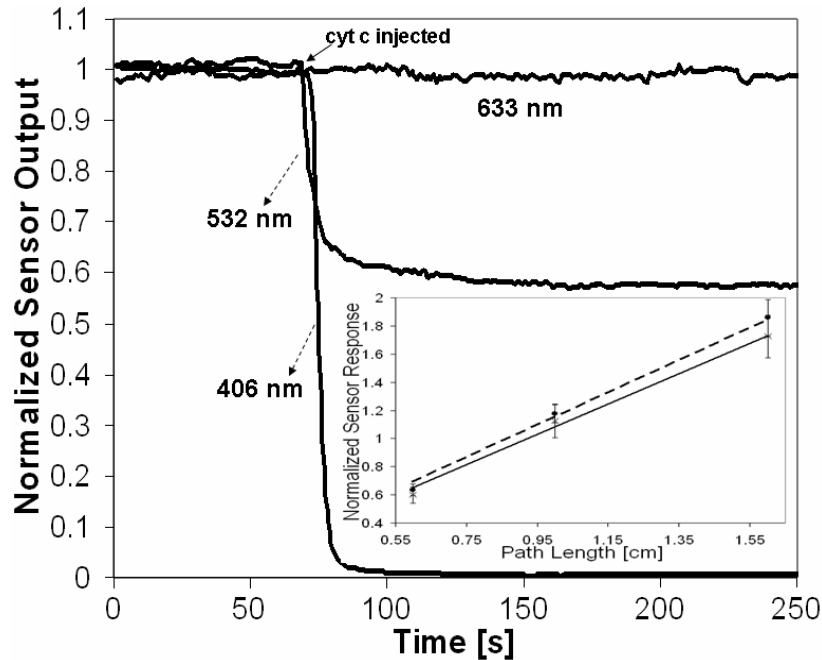


Fig. 3. Experimental data showing the response of the sensor to about one half of a monolayer of cyt c. The inset shows the normalized sensor response ($A/(\epsilon \kappa)$) with respect to the probing path length at 406 nm (dashed line) and at 532 nm (solid line). The SNR is measured to be ~ 1500 for 406 nm laser source.

The inset in Fig. 3 shows the normalized sensor response with respect to pathlength for the two wavelengths (406 and 532 nm). The normalized sensor response is defined as $A/(\epsilon \kappa)$. The lines are the best linear fits to the experimental data points. The normalized response is very similar at the two wavelengths and there is no significant deviation from a linear dependence as the pathlength increases, thus indicating that stray light did not degrade the measurements and spectroscopic response was achieved as expected.

To investigate the adsorption isotherm of cyt c onto the glass waveguide surface we prepared solutions with different concentrations and measured the optical absorbance near the Soret band (406 nm). Figure 4 shows the adsorption isotherm of cyt c onto the glass waveguide surface from phosphate buffer solutions at pH-7. The x-axis shows the bulk concentration of cyt c in the sensing region, and y-axis shows the optical absorbance on the left and the corresponding surface concentration on the right. After injection of cyt c we waited for 10 minutes for stabilization before taking these measurements. The experiment was repeated three times to measure the optical absorbance and determine the surface concentration for a given volume concentration. Between each measurement, the probing surface was prepared as described in the surface preparation section to provide exactly the same physical/chemical environment. However, it is well-known that the physical/chemical environment near the surface (i.e. temperature, pH) can affect the temporal behavior of the adsorption process, the final amount of surface-adsorbed molecules, and also the Soret absorption band for cyt c molecules [11, 22]. The variability on the final concentration of surface-adsorbed molecules was quantified by the error bars in Fig. 4. These error bars are the standard deviation of three independent measurements and they quantify our ability (or lack of) to reproduce the same surface concentration of adsorbed molecules with identical optical properties; it is a consequence of the variations on the surface environment.

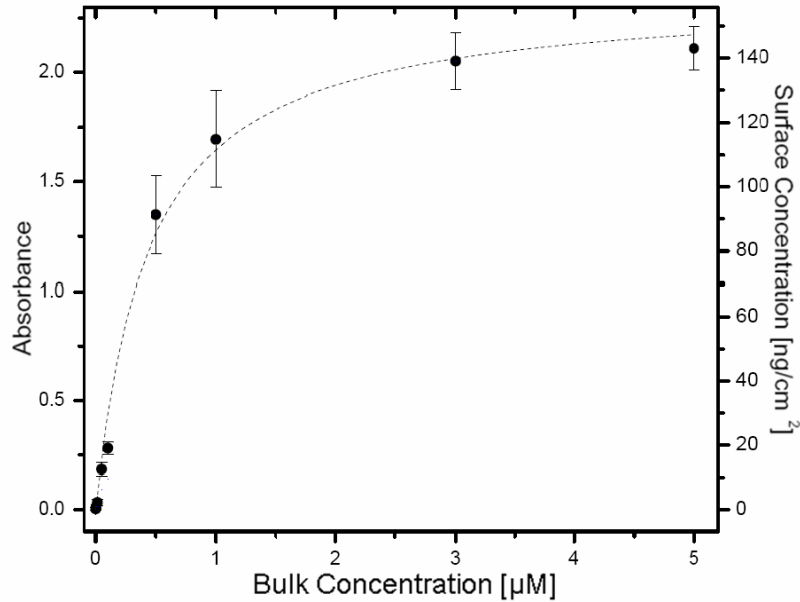


Fig. 4. Adsorption isotherm of cyt c on the glass surface at pH-7, measured at 406 nm. The dashed curve is the best fit of the experimental data to a Langmuir adsorption model with $K_a = 2.4 \times 10^6 \text{ M}^{-1}$. The error bars are showing the surface concentration variance of independent three measurements.

As shown in Fig. 4, the surface coverage gradually levels off as the bulk concentration increases above 3 μM . The dashed line is the best fit of the experimental data to a Langmuir adsorption isotherm

$$\Theta = \frac{K_a C_b}{1 + K_a C_b} \quad (2)$$

where Θ is the ratio of the number of occupied adsorption sites to the total number of sites at saturation and K_a is the adsorption equilibrium constant. This constant is strongly dependent on the surface chemistry of the substrate [11]. The observation of a saturation regime as in Fig. 4 is another indication that the detected signals originated from surface-bound proteins rather than free protein molecules dissolved in the aqueous solution [11]. The equilibrium constant for Corning 0211 glass surface was found to be $K_a = 2.4 \times 10^6 \text{ M}^{-1}$ and this value is almost equal to the equilibrium constant, $K_a = 2.5 \times 10^6 \text{ M}^{-1}$, that was determined by using the cyt c adsorption data given in Table 1 of Ref. [23] for indium tin oxide surfaces.

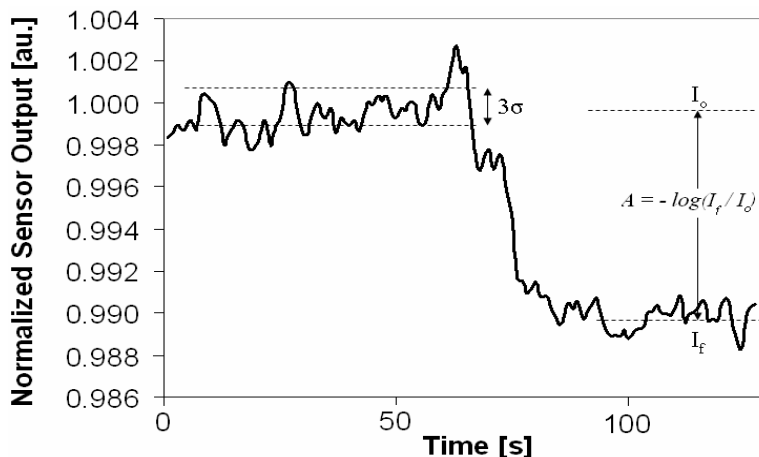


Fig. 5. Response of the sensor to 1 nM of cyt c solution. This corresponds to about 270 pg/cm^2 surface coverage. The signal change is $I_0 - I_f \approx 0.01$, which in absorbance units corresponds to $A = -\log(0.99) \approx 4 \times 10^{-3}$, well above than the $A_{\text{LOD}} = 8.69 \times 10^{-4}$.

Figure 5 shows the normalized device response to 1 nM of cyt c solution at 406 nm. The calculated root-mean square (RMS) noise value from the figure is $\sigma \approx 6.7 \times 10^{-4}$, in the time scale of one minute. The SNR of our measurements was calculated to be $(I_0 / \sigma) = 1.5 \times 10^3$, where I_0 is the time average of the normalized waveguide output before cyt c is introduced to the surface. The LOD can be calculated from the RMS noise value by using the standard assumption in analytical measurements that one can detect changes that are three times larger than the noise level ($3\sigma = 2 \times 10^{-3}$, in our case). In absorbance units a change of 3σ corresponds to $A_{\text{LOD}} = -\log(I_{\text{LOD}} / I_0) = -\log(1 - 3\sigma) = 8.69 \times 10^{-4}$. This value is an order of magnitude better compared to previously reported values [7]. When we consider that a surface coverage of 140 ng/cm^2 causes an optical absorbance of 2.1 as determined in Figs. 3 and 4, our detection limit can be calculated to be about 59 pg/cm^2 . This LOD is below the range typically quoted for state-of-the-art SPR equipment and besides that these SPR data can only be obtained through extremely high experimental precision and environmental control. In Fig. 5, the 1 nM of cyt c solution causes an absorbance of about $A = -\log(I_f / I_0) = 4 \times 10^{-3}$, which corresponds to a protein surface coverage of 270 pg/cm^2 .

6. Conclusion

In conclusion, we have presented a simple and robust integrated optic sensing platform based on silver film ion-exchange waveguides; those waveguides exhibit high sensitivity and sufficiently low losses to operate in the single-mode regime in the wavelength range of 400-650 nm. By taking advantage of the extremely high extinction coefficient at the Soret band present in heme proteins, we probed surface adsorption of protein films at glass/water interfaces. We presented the adsorption isotherm of oxidized cyt c protein films on the waveguide borosilicate glass surface and reported a value smaller than 100 pg/cm^2 for the limit of detection. The highly sensitive and spectroscopic selective detection of protein films described here can potentially become an important bioanalytical tool for monitoring protein binding at several biomimetic surfaces in technologies such as high-throughput screening of novel pharmaceutical drugs and immuno-assay biosensors.

Acknowledgments

The authors would like to acknowledge support from National Science Foundation grant numbers DMR-0099862 (to NP) and DBI 0352449 (to SBM), and also the state of Arizona TRIF program.